Journal of Cellular Biochemistry 95:1235–1247 (2005)

Topoisomerase Inhibitor Induced Dephosphorylation of H1 and H3 Histones as a Consequence of Cell Cycle Arrest

Nicole Happel,* Arne Sommer, Kristina Hänecke, Werner Albig, and Detlef Doenecke

Institute for Biochemistry and Molecular Cell Biology, University of Göttingen, Humboldtallee 23, 37073 Göttingen, Germany

Abstract Posttranslational modifications of histones have an integral function in the structural and functional organization of chromatin. Several changes in the modification state of histones could be observed after induction of apoptosis with topoisomerase inhibitors and other inducers. Most of these studies include the analysis of the state of phosphorylation of histones, and the results are to some extent controversial, depending on cell lines and agents used. In the present study we compared the kinetics of the dephosphorylation of H1 and H3 histones with apoptosis markers after treatment of leukemic cell lines with topoisomerase inhibitors. In parallel, we determined cell cycle parameters in detail. Dephosphorylation of both histone classes started within 1 h of induction, and no direct correlation with timing and intensity of the investigated apoptotic features could be observed. In contrast, we show that the effect of topoisomerase inhibitors on the state of H1 and H3 phosphorylation is not directly related to apoptosis, but reflects the changes in the cell cycle distribution of cells treated with these inducers. J. Cell. Biochem. 95: 1235–1247, 2005. © 2005 Wiley-Liss, Inc.

Key words: histone; apoptosis; topoisomerase inhibitor; cell cycle; phosphorylation; capillary zone electrophoresis

In eukaryotes, DNA is organized as a nucleoprotein complex termed chromatin. The basic unit of chromatin is the nucleosome, consisting of an octamer of two of each of the four core histones H2A, H2B, H3, and H4, one linker histone H1 and about 200 bp of DNA [Khorasanizadeh, 2004]. All histone classes, except H4, consist of several subtypes. These histones mediate the compaction of the DNA within the nucleus and are important for the regulation of genome function [reviewed in Horn and Peterson, 2002; Felsenfeld and Groudine, 2003]. The histones are targets of several types of covalent modifications including acetylation, methylation, ubiquitination, sumoylation, and phosphorylation [Grant, 2001; Shiio and Eisenman, 2003]. According to the so called histone code hypothesis, the histones and their covalent modifications contribute to a mechanism that can alter chromatin structure and thereby regulate gene expression or define specific higher order structures [Strahl and Allis, 2000; Jenuwein and Allis, 2001]. The number of described modification sites is continuously growing, but in just few cases the functional implications of their modifications are known. Particularly, the influence of the histone modifications during the apoptotic chromatin changes has hardly been investigated. Most frequently, a change of the phosphorylation state of the histones during apoptosis was observed but the results are to some extent controversial, depending on the cell line and on the agent used to induce apoptosis [reviewed in Th'ng, 2001].

Recently, we have demonstrated a dephosphorylation of H1 histones during apoptosis induced with the camptothecin derivative topotecan, an inhibitor of the topoisomerase I and the kinase inhibitor staurosporine, respectively

Abbreviations used: CZE, capillary zone electrophoresis; PAGE, polyacrylamide gel electrophoresis; Ser10, serine 10; Ser28, serine28; AFC, 7-amino-4-trifluoromethylcoumanin.

Grant sponsor: Deutsche Forschungsgemeinschaft (DFG); Grant number: Do143/19-1/2.

*Correspondence to: Dr. Nicole Happel, Institute for Biochemistry and Molecular Cell Biology, Humboldtallee 23, 37073 Göttingen, Germany. E-mail: nhappel@gwdg.de

Received 23 November 2004; Accepted 7 March 2005

DOI 10.1002/jcb.20494

[Kratzmeier et al., 2000]. In the present study, we have extended the analysis to H3 histones and have included an additional cell line (Jurkat) and the topoisomerase II inhibitor etoposide in addition to the topoisomerase I inhibitor topotecan.

Among other effects, the phosphorylation of the H1 as well as of the H3 histones is correlated to the cell cycle [Loury and Sassone-Corsi, 2003]. The H1 subtypes are progressively phosphorylated during the cell cycle and this modification becomes maximal during late G2 and mitosis [Bradbury et al., 1973, 1974; Hohmann et al., 1976; Boggs et al., 2000]. The number of attached phosphate groups increases from zero to three in late S-phase up to five to six at the G2/M transition [Langan et al., 1981; Talasz et al., 1996]. H3 histones are highly phosphorylated by the Aurora-B kinase at Ser10 and Ser28 during mitosis, but the function of these phosphorylations is not completely elucidated [Goto et al., 2002; Sugiyama et al., 2002; Prigent and Dimitrov, 2003].

Here we show that the dephosphorylation of H1 and H3 histones as observed after apoptosis induction is not correlated with the timing and intensity of the investigated apoptotic features. In contrast, we demonstrate a correlation of the dephosphorylation of both histone classes with a change in the cell cycle distribution of leukemic cell lines after treatment with topoisomerase inhibitors.

MATERIALS AND METHODS

Cell Culture

The human leukemic cell line HL60 was cultured as described previously [Kratzmeier et al., 2000]. The human leukemic cell line Jurkat (DSMZ no. ACC 282) was obtained from the DSMZ (Braunschweig, Germany). Jurkat cells were cultured in RPMI-1640 medium (Biochrom KG, Berlin, Germany) supplemented with 1% glutamine and 10% fetal calf serum (FCS, Biochrom KG, Berlin, Germany) in a humidified 5% CO_2 atmosphere.

Induction of Apoptosis and Cell Cycle Arrest

To induce apoptosis, both cell lines HL60 and Jurkat were treated with topotecan (final concentration 328 nM; stock solution dissolved in H_2O; GlaxoSmithKline, München, Germany) or etoposide (final concentration 20 μM; stock solution dissolved in EtOH; Sigma, Taufkirchen, Germany) for various times as indicated in the figures. To accumulate HL60 cells in different cell cycle phases, cells were incubated with aphidicolin (1.5 μM for 24 h; Qbiogene-Alexis, Grünberg, Germany), 5-fluorouracil (20 μM for 24 h; Sigma) or nocodazole (1.33 μM for 12 h; Sigma) as indicated in the figures.

Assays for Apoptosis Detection

The process of ongoing apoptosis was monitored by light microscopy and also by the isolation of fragmented DNA from apoptotic cells as described previously [Kratzmeier et al., 1999]. The fragmented DNA from equal numbers of cells was applied onto a 1.5% agarose gel and separated electrophoretically.

In addition, the protease activity of caspase-3 was measured according to the method of Thornberry [1994] as described by Meergans et al. [2000] with the following modifications: 10 μl of cytosolic extracts were mixed with 90 μl substrate buffer (50 μM fluorogenic substrate AcDEVD-AFC (Biosource, Camarillo, USA) in 50 mM HEPES, pH 7.5, 1% sucrose, 0.1% CHAPS, 10 mM dithiothreitol). Blanks contained 10 μl of extraction buffer and 90 μl of substrate buffer. Generation of free AFC was determined by fluorescence measurement at $t = 0/t = 20$ min using the Fluoroskan Ascent FL (Labsystems, Frankfurt, Germany) set at an excitation wavelength of 390 nm and an emission wavelength of 510 nm.

Purification of Histone Proteins From Human Tumor Cell Lines

For the purification of H1 histones cells (usually 5×10^7 cells/incubation) were harvested by centrifugation (5 min, room temperature, 300*g*) and washed once with phosphate-buffered saline. Perchloric acid (0.83 M) was added to the cell pellet, and cells were lysed and extracted by incubation for 1 h on ice. Samples were centrifuged (10 min, 4°C, 14,000*g*) and the acid-soluble proteins in the supernatant were precipitated with a final concentration of 20% TCA for 1 h. After centrifugation (30 min, 4°C, 14,000*g*), the pellet was washed with cold (−20°C) acetone and air-dried. The histones were dissolved in 30 mM HCl. The purification of core histones was done in the same way with the exception that the cell pellet was extracted with 0.2 M sulfuric acid instead of 0.83 M perchloric acid.

Immunoblotting

Core histones were separated on a 15% SDS-polyacrylamide gel and electrophoretically transferred to nitrocellulose. Blots were probed with phospho-histone H3 (Ser10) antibody (no. 9701; CST, New England Biolabs, Frankfurt, Germany) in a 1:1,000 dilution or phospho-histone H3 (Ser28) antibody (no. 07-145; Upstate, Charlottesville, USA) in a 1:500 dilution. After incubation with a horseradish peroxidase-conjugated goat anti-rabbit antibody (no. A0545; Sigma), the immunoreactive proteins were visualized using the chemiluminescence ECL plus detection system (Amersham Bioscience, Freiburg, Germany). To confirm equal amounts of histone H3 in each lane, blots were stripped and probed with a histone H3 antibody (no. 9715; CST) followed by alkaline phosphatase-conjugated goat anti-rabbit antibody (no. 111-055-045, Dianova, Hamburg, Germany).

CZE of H1 Histones

CZE was performed on a P/ACE MDQ system (Beckman Coulter, Fullerton, USA). The separation conditions are described in Kratzmeier et al. [2000]. The capillary type was fused silica with 110 cm length, and an inner diameter of 50 μm. Separations were performed at the following conditions: temperature, 30°C; voltage, 18.3 kV; separation time, 60 min; sample injection by pressure; injection time, 10 s; sample protein concentration, ~0.5 mg/ml; absorbance detection at 200 nm. Separation buffer was 30 mM H_3PO_4, 60 mM $HClO_4$, 0.02% hydroxypropylmethylcellulose, pH 2.0, adjusted with triethylamine.

Flow Cytometry

To estimate the cell cycle distribution, control and treated cells (1×10^6 cells) were fixed in 70% ethanol at −20°C and washed with PBS. Further preparation was done with the CycleTest Plus DNA Reagent Kit according to the instructions provided (no. 340242; BD Bioscience, San Jose, USA) and samples were subjected to a FACSCalibur Flow Cytometer (BD Bioscience). Cell cycle distribution was analyzed using the software Modfit LT (Verity Software House, Topsham, USA).

For staining of cdc2 phosphorylated at Tyr15 control and treated cells were fixed in 70% methanol at −20°C. Cells were then centrifuged (500*g*, 4°C, 5 min), rinsed once with PBS/1% BSA, centrifuged again, and resuspended in 1 ml PBS/0.25% Triton X-100. Cells were kept on ice for 5 min, then 3 ml PBS were added and centrifuged again. The cells were washed twice with PBS/1% BSA and then resuspended in 100 μl PBS/1%BSA, containing the phospho-cdc2 (Tyr15) antibody (no. 9111; CST) in a 1:100 dilution. As isotype control normal rabbit IgG (no. NI01; Oncogene, San Diego, USA) was used. After overnight incubation at 4°C, the cells were rinsed twice with PBS/1% BSA and then resuspended in 100 μl of PBS/1% BSA containing Alexa Fluor 488 $F(ab')_2$ fragment of goat anti-rabbit IgG antibody (no. A11070, Molecular Probes, Eugene, USA) in a 1:400 dilution. A 45 min incubation at room temperature followed, after which the cells were washed twice with PBS/1% BSA. The DNA was stained by suspending the cells in 500 μl PBS containing 100 μg/ml RNase A and 50 μg/ml propidium iodide. After an incubation of 30 min at room temperature cells were measured with a FACSCalibur Flow Cytometer (BD Bioscience). Analysis was done using the software WinList (Verity Software House).

Immunofluorescence Microscopy

To estimate the amount of M-phase cells, control and treated cells were fixed with cold (−20°C) methanol and stained with the DNA fluorochrome 4′-6-diamidine-2-phenyl indole (DAPI) using Vectashield Mounting Medium with DAPI (Vector Laboratories, Burlingame, USA). At least 1,000 cells were screened under a fluorescence microscope (Axioskop, Zeiss, Göttingen, Germany) and cells with mitotically condensed chromatin (prophase to telophase) were counted.

RESULTS

Topoisomerase Inhibitor Induced Dephosphorylation of H3 Histones

To investigate the state of phosphorylation of the H3 histones after induction of apoptosis, Jurkat and HL60 cells were treated with the topoisomerase inhibitor topotecan or HL60 cells were treated with the topoisomerase II inhibitor etoposide. Histones were extracted at different times after induction and the phosphorylation of H3 histones was analyzed using antibodies

specific for phospho-histone H3 (Ser10) and phospho-histone H3 (Ser28). The progression of apoptosis was followed by analyzing oligonucleosomal DNA fragmentation and the activity of caspase-3.

After induction of HL60 cells with topotecan, an increasing oligonucleosomal DNA fragmentation and an increase of the caspase-3 activity was observed 2 h after induction (Fig. 1A,B, HL60 + topotecan). This apoptotic response of HL60 cells to topoisomerase I inhibitors has previously been demonstrated by us [Kratzmeier et al., 1999] and by other groups [Kantarjian, 1999]. A rapid dephosphorylation of H3 at Ser10 as well as at Ser28 started in the first hour after induction. Six hours after induction of the cells with topotecan phosphorylation at Ser10 and Ser28 was decreased below the limit of detection (Fig. 1C).

Jurkat cells treated with topotecan also showed a rapid dephosphorylation of the histones H3 at Ser10 and Ser28 (Fig. 1C; Jurkat + topotecan). Apoptotic characteristics were first observed after 4 h through an increase of caspase-3 activity (Fig. 1A,B). Six hours after induction, there was a strong apoptotic signal for the chromatin fragmentation (Fig. 1A) and caspase-3 activity (Fig. 1B).

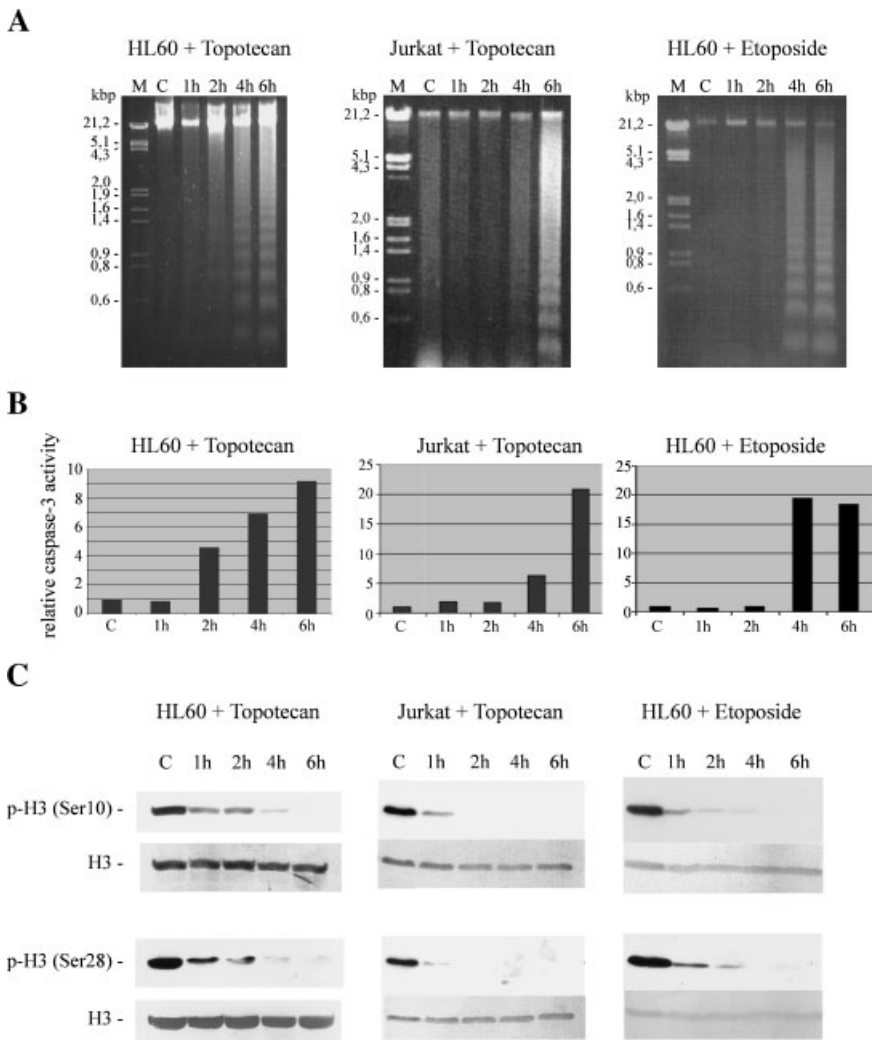

Fig. 1. Dephosphorylation of H3 histones after treatment of HL60 and Jurkat cells with topoisomerase inhibitors. HL60 and Jurkat cells were treated with 328 nM topotecan or HL60 cells were treated with 20 μM etoposide for 1, 2, 4, and 6 h. Fragmented DNA was isolated (**A**). The DNA size marker (M) was lambda DNA/EcoRI + HindIII from MBI with fragments between 21,226 bp and 564 bp. Caspase-3 activity was measured in cell lysates using the colorimetric substrate DEVD-AFC (**B**). Core histones were purified as described and equal protein amounts were separated by 15% SDS-PAGE and immunoblotted with phospho-H3 (Ser10) antibody (p-H3 (Ser10)), phospho-H3 (Ser28) (p-H3 (Ser28)), and H3 antibody (**C**).

In a second series of experiments, we treated HL60 cells with the topoisomerase II inhibitor etoposide. This also resulted in a rapid dephosphorylation of the H3 histones. The effect on H3 phosphorylation was observed during the first hour after induction and its progression was faster than in case of the topotecan treatment (Fig. 1C; HL60 + etoposide). The apoptotic markers were not positive until 4 h after induction and then they abruptly turned to high intensity (Fig. 1A,B).

In all the three assays, the dephosphorylation of H3 at Ser10 and Ser28 started in the first hour after induction. In these cases, no correlation in timing and intensity with the detectable activation of apoptotic markers could be observed.

Correlation Between the H3 Dephosphorylation and the Decrease of M-phase Cells After Treatment With Topoisomerase Inhibitors

Because of the known association between the phosphorylation state of the H3 histones and the M-phase of the cell cycle, we analyzed whether the dephosphorylation of H3 histones observed after treatment with topoisomerase inhibitors was caused by a decrease of mitotic cells. For this reason, we counted under the microscope the cells with mitotically condensed chromatin, i.e., cells from prophase to telophase, after DAPI-staining. We then compared this distribution with the state of dephosphorylation of the H3 histones at Ser10 and Ser28. With all the three assays (HL60 cells with topotecan or etoposide, Jurkat cells with topotecan), a dramatic decrease of the number of mitotic cells could be observed that corresponded to the dephosphorylation of the H3 histones at Ser10 and Ser28 (Fig. 2). Two hours after induction, the decrease of the phosphorylation at Ser10 was slightly slower than that of Ser28. This can be explained by the fact that the mitotically linked phosphorylation of H3 at Ser10 can be found from late G2 to metaphase and at Ser28 for a shorter time, namely, from prophase to metaphase [Goto et al., 2002].

We further confirmed our results in case of the topotecan treated Jurkat cells, where a rapid decrease of the H3 phosphorylation in the first hour of induction had been observed (Fig. 1C), by analyzing the share of cdc2 phosphorylated at Tyrosine 15 (Tyr15). This phosphorylation inhibits the activity of the cdc2

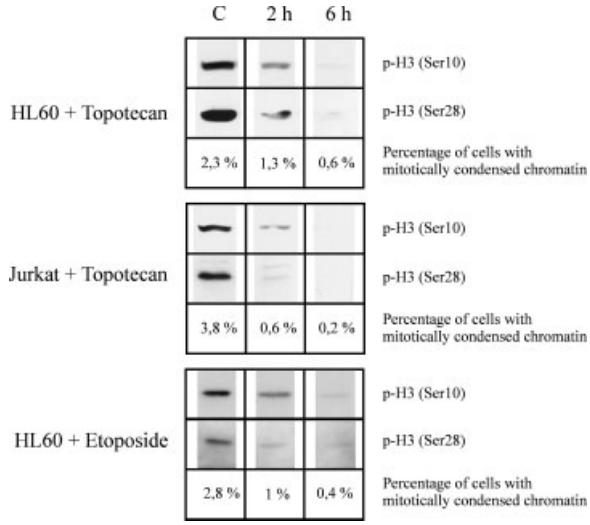

Fig. 2. Comparison of H3 phosphorylation with percentage of cells with mitotically condensed chromatin. HL60 cells and Jukat cells were treated with 328 nM topotecan or HL60 cells were treated with 20 μM etoposide for 2 and 6 h or were not induced (control, C). Core histones were extracted and immunoblots with phospho-H3 (Ser10) and phospho-H3 (Ser28) antibody were carried out. From the same experiment cells were stained with the DNA binding fluorochrome DAPI and at least 1,000 cells were examined by fluorescence microscopy and cells with mitotically condensed chromatin (prophase to telophase) were counted.

kinase that is necessary for the entry into the M-phase [Norbury et al., 1991].

We treated Jurkat cells with topotecan for 1 and 2 h, and determined the DNA content and the phosphorylation of cdc2 at Tyr15 by flow cytometry (Fig. 3). The analysis of G2/M phase cells in the control revealed two populations regarding the phosphorylation of cdc2 at Tyr15. One small portion of the cells was negative in relation to this phosphorylation. These are the M-phase cells. The main portion of the cells was positive in respect to this phosphorylation at Tyr15, they represent the cells in G2 (Fig. 3C, control). One hour after induction of Jurkat cells with topotecan, there was an obvious loss of cells with cdc2 dephosphorylated at Tyr15 demonstrating the decrease of M-phase cells (Fig. 3C, 1 h). A further decrease of cells with cdc2 dephosphorylated at Tyr15 could be observed 2 h after induction (Fig. 3C, 2 h). Together these results show an arrest at G2/M transition after topotecan treatment, and thus a clear relationship between the decrease of the rate of M-phase cells and the dephosphorylation of H3 at Ser10 and Ser28 after apoptosis induction with topoisomerase inhibitors.

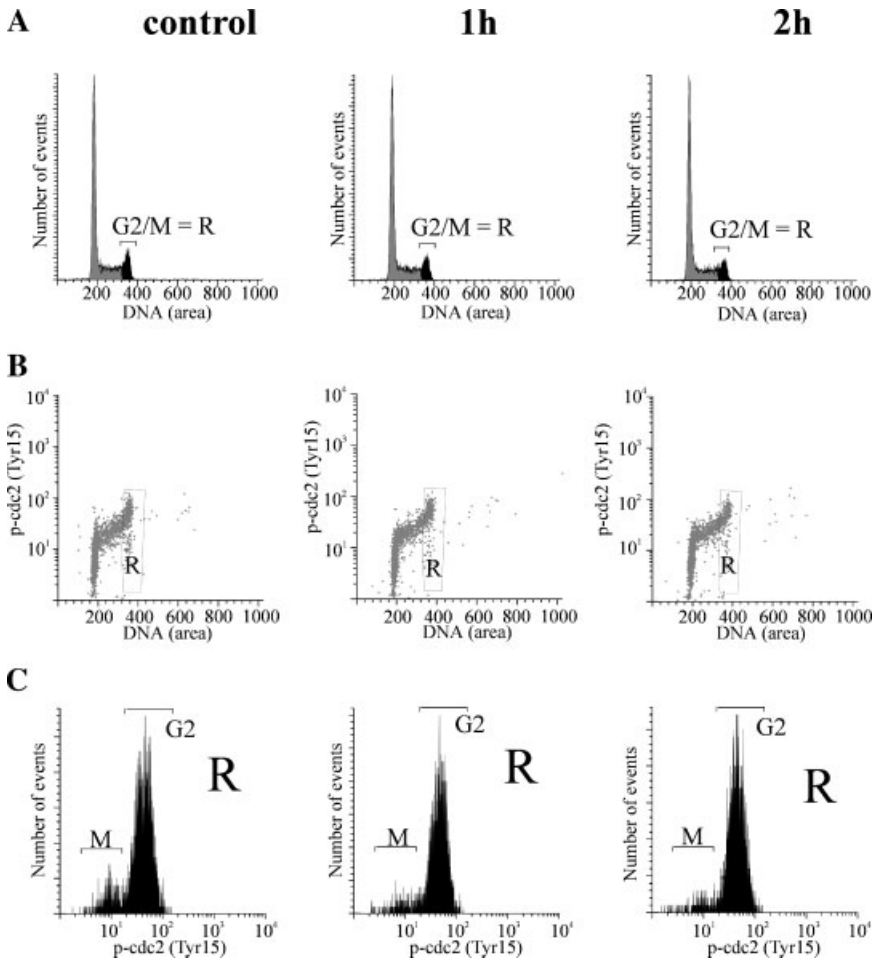

Fig. 3. Cell cycle arrest in G2 after topotecan treatment. After treatment of Jurkat cells with 328 nM topotecan for 1 and 2 h (untreated cells = control) they were analyzed by flow cytometry. Cells were double-labeled with propidium iodide to analyze the cell cycle profile and with an antibody specific for cdc2 phosphorylated at tyrosine 15 (p-cdc2 (Tyr15)). The cell cycle distribution was displayed (**A**) and a gate (R) was set around the G2/M cells. A plot of the cell cycle distribution vs. p-cdc2 (Tyr15) is shown in (**B**). The squares (R) enclose the gated G2/M cells. The p-cdc2 (Tyr15) fluorescence histogram of the gated G2/M cells is shown in (**C**). The p-cdc2 (Tyr15)-negative portion represents the M-phase cells, while cells in G2 are positive for p-cdc2 (Tyr15).

Dephosphorylation of H1 Histones as a Result of a Change of the Cell Cycle Distribution After Apoptosis Induction With Topoisomerase Inhibitors

We have previously described the dephosphorylation of H1 histone subtypes after topotecan treatment of HL60 cells [Kratzmeier et al., 2000]. Now we have investigated the phosphorylation state of the H1 histones of HL60 cells after treatment with etoposide and of Jurkat cells after induction with topotecan so as to compare these results with the kinetics of the H3 histone dephosphorylation.

The phosphorylation state of the H1 histones was analyzed using CZE. The migration time of

Fig. 4. Comparison of the H1 dephosphorylation and the cell cycle distribution after apoptosis induction with topoisomerase inhibitors. HL60 and Jurkat cells were treated with 328 nM topotecan and HL60 cells treated with 20 μM etoposide for 2 and 6 h or were not induced (control). H1 histones were purified by perchloric acid extraction and subjected to CZE using fused silica capillary. Absorbance data at 200 nm were continuously recorded (**A**, **C**, **E**). The identities of the peaks within the total H1 pattern with the three main H1 subtypes (H1.2, H1.4, and H1.5) and their monophosphorylated forms (p-H1.2, p-H1.4, and p-H1.5) are indicated with arrows as described previously [Kratzmeier et al., 2000]. The higher phosphorylated forms comigrate with the H1.2 and p-H1.2 peaks and even at later migration times. The cell cycle distribution was measured by flow cytometry and data were analyzed using the software Modfit LT from Verity (**B**, **D**, **F**). The percentage distribution in the different phases of the cell cycle is given by numbers in the graphs. For example: HL60 untreated control cells with 36% in G1-phase, 47% in S-phase, and 17% in G2/M-phase (36/47/17).

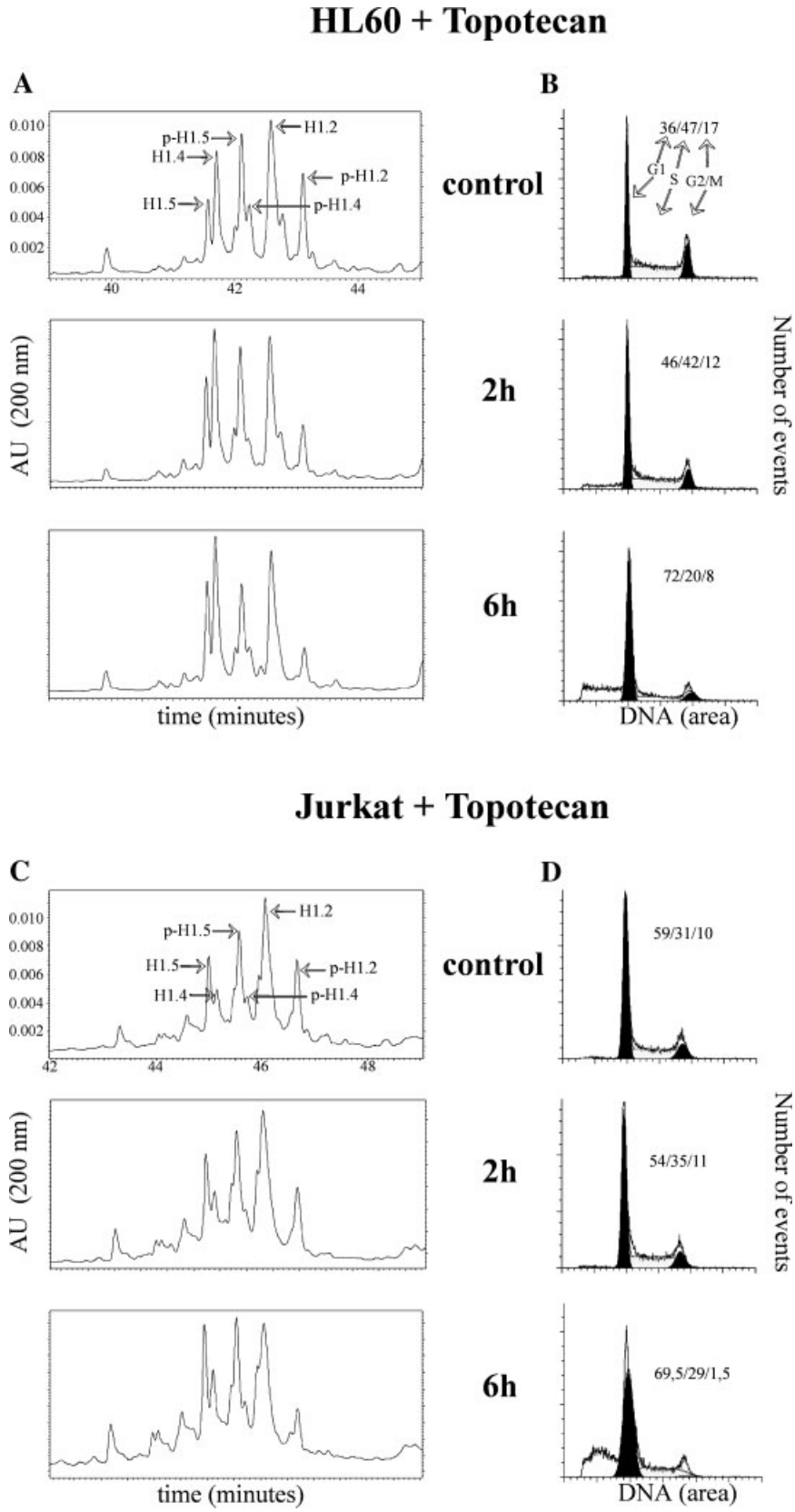
HL60 + Topotecan
A
B
p-H1.5
H1.4
H1.2
p-H1.2
H1.5
p-H1.4
control
36/47/17
G1
S
G2/M
2h
46/42/12
6h
72/20/8
AU (200 nm)
Number of events
time (minutes)
DNA (area)
Jurkat + Topotecan
C
D
control
59/31/10
2h
54/35/11
6h
69,5/29/1,5
AU (200 nm)
Number of events
time (minutes)
DNA (area)

Fig. 4.

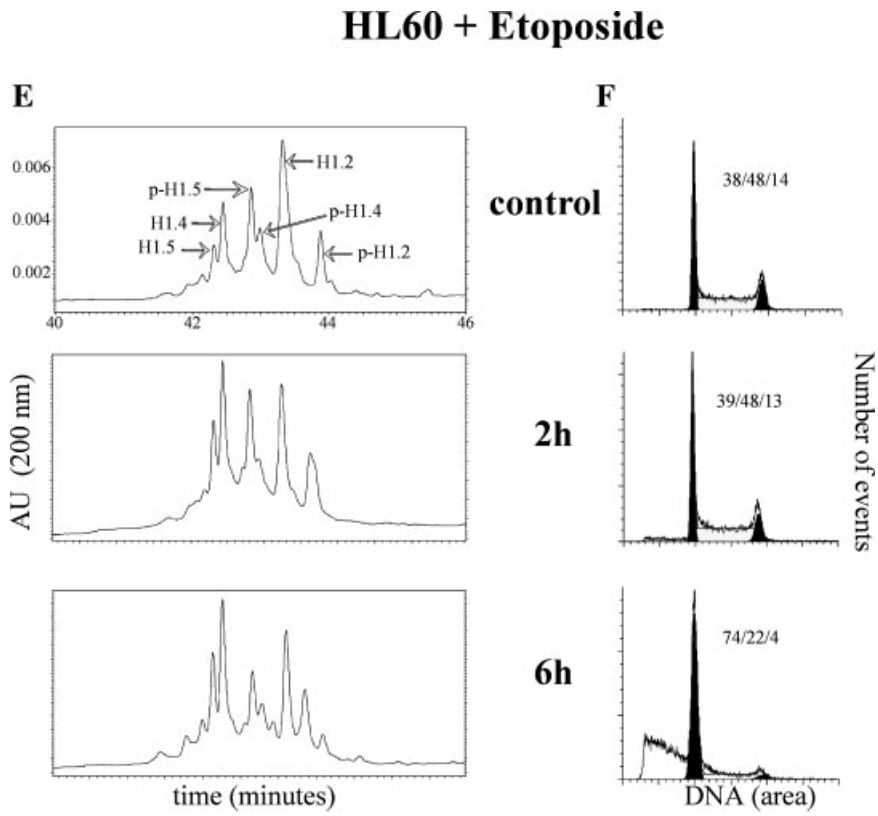

Fig. 4. (*Continued*)

the H1 histones increases with the number of phosphate groups. Thus, the electrophorectic mobility of the H1 histones is higher after dephosphorylation, and a general dephosphorylation of the H1 histones results in a shift of the peaks to the left, i.e., towards shorter migration times [Kratzmeier et al., 2000].

After induction with both topotecan or etoposide, the HL60 cells reacted with a dephosphorylation of the H1 histones (Fig. 4A,E). Jurkat cells also showed a dephosphorylation of the H1 histones after induction with topotecan (Fig. 4C). However, the progression was much slower than in the case of the HL60 cells. In addition, these data show that in analogy to the H3 phosphorylation state, the kinetics of H1 histone dephosphorylation and the activation of markers of apoptosis, i.e., DNA fragmentation and caspase-3 activation (Fig. 1), are not tightly correlated.

To determine if the observed dephosphorylation of the H1 histones also results from changes in the cell cycle phase distribution, we analyzed the cell cycle distribution of the treated HL60 and Jurkat cells. It is known that the H1 subtypes are progressively phosphorylated during the cell cycle and this modification becomes maximal during late G2 and mitosis [Bradbury et al., 1973, 1974; Hohmann et al., 1976; Boggs et al., 2000]. The number of attached phosphate groups increases from zero to three in late S-phase up to five to six at the G2/M transition [Langan et al., 1981; Talasz et al., 1996]. It should be kept in mind that the CZE electropherograms are an overlay of patterns from the H1 histones with various phosphorylation levels extracted from the cells in the different cell cycle phases.

The determination of the DNA content by flow cytometry revealed that the HL60 cells, both after induction with topotecan as well as with etoposide, showed a significant loss of S- and G2/M-phase cells during the 6 h after induction (Fig. 4B,F). In case of the Jurkat cells, a strong decrease of the amount of G2/M-phase could be observed 6 h after induction with topotecan, but in contrast to the HL60 cells, no major change in the amount of the S-phase cells occurred (Fig. 4D). It can be concluded that the HL60 cells showed a more rapid dephosphorylation of the H1 histones than the Jurkat cells because of the decrease of S-phase and G2 cells in addition

to M-phase cells. In contrast, in case of the Jurkat cells, there was just a small change in the share of the S-phase cells and, therefore, just a gradual dephosphorylation of H1 histones occurred.

Thus, the dephosphorylation of the H1 histones shown by the shift of the peaks of the CZE electropherograms towards shorter migration times is mainly correlated to the loss of S-phase cells after apoptosis induction with topoisomerase inhibitors.

To further substantiate the strong correlation of the observed CZE H1 histone patterns with the cell cycle distribution, we analyzed the H1 phosphorylation state with CZE after arresting HL60 cells in the different phases of the cell cycle and compared this with the H1 phosphorylation pattern resulting from topotecan treatment.

Treatment of HL60 cells with aphidicolin, an inhibitor of DNA polymerase α, δ, and ε [Cheng and Kuchta, 1993; Yamada and Itoh, 1994], resulted in an accumulation of G1 and S-phase cells (Fig. 5, aphidicolin). The H1 histones of these cells were less phosphorylated than from the untreated control cells, but they were more phosphorylated than after apoptosis induction with topotecan (Fig. 5, aphidicolin, topotecan). This higher level of phosphorylation of the H1 histones after aphidicolin treatment resulted from the portion of S-phase cells, as demonstrated by the comparison with the H1 pattern from the cells blocked with the antimetabolite 5-fluorouracil in S-phase [Longley et al., 2003] (Fig. 5, fluorouracil). Because of the loss of S-phase cells from the apoptotic topotecan treated cells, the H1 histones are less phosphorylated than after aphidicolin treatment. The arrest of HL60 cells in M-phase using nocodazole, which inhibits the dynamics of microtubules [Jordan et al., 1992], leads to the expected hyperphosphorylation of the H1 histones (Fig. 5, nocodazole).

We also checked whether the treatment with these agents induces apoptosis. Only nocodazole induced apoptosis in HL60 cells, whereas neither after aphidocolin nor after 5-fluorouracil treatment apoptotic features could be detected (data not shown). This indicates that we can be sure that the observed dephosphorylation after G1/S and S-phase arrest resulted from the changed cell cycle distribution.

From our results we can conclude that the observed dephosphorylation of the H1 as well as of the H3 histones is not directly connected to the apoptotic process but is a consequence of the change of the cell cycle distribution after treatment of the leukemic cells with topoisomerase inhibitors.

DISCUSSION

Apoptotic cells undergo typical morphological and physiological changes. One hallmark of apoptotic cells is the condensation and fragmentation of chromatin [Rogalinska, 2002]. The molecular details of these dynamic structural changes in the cell nucleus are still unclear. It is, however, conceivable that a major role in these structural transitions is played by the histones and their reversible posttranslational modifications.

So far, there are only few investigations about histone modifications during the apoptotic chromatin condensation and fragmentation. In these studies, the phosphorylation state of the histones was most frequently investigated [reviewed in Th'ng, 2001; Loury and Sassone-Corsi, 2003]. The only core histone modification that seems to be uniquely associated with apoptosis is the histone H2B phosphorylation, which appears to be important for the chromatin fragmentation [Ajiro, 2000; Cheung et al., 2003]. A phosphorylation of H2A.X is induced by DNA-double strand breaks and also by apoptosis as triggered, for example, by anti-Fas antibodies. It is discussed that this histone modification is important for the packaging of fragmented DNA into apoptotic bodies [Rogakou et al., 1998, 2000; reviewed in Pilch et al., 2003]. The results regarding the phosphorylation state of the H1 and H3 histones after apoptosis induction are to some extent controversial, depending on the cell line and on the method used for apoptosis induction [reviewed in Th'ng, 2001].

In a previous study, we were able to show a rapid dephosphorylation of H1 histones after apoptosis induction with the topoisomerase I inhibitor topotecan [Kratzmeier et al., 2000]. Here we could show, using modification specific antibodies for H3 histone phosphorylated at Ser10 or Ser28, respectively, and capillary zone electrophoresis, that both the H3 histones and the H1 histones were dephosphorylated after apoptosis induction by inhibition of the topoisomerase I or II. Surprisingly, the kinetics of both histone dephosphorylations were not

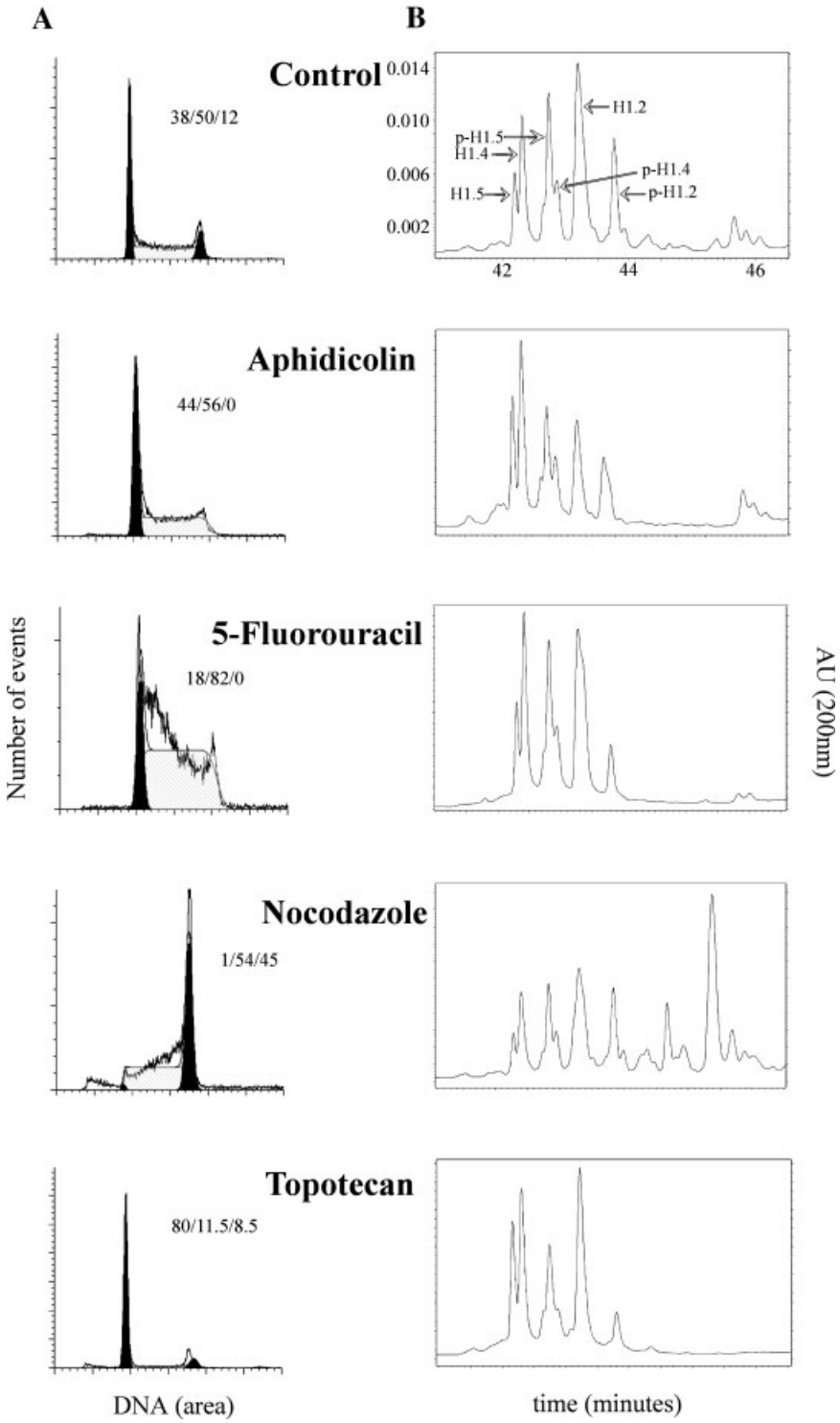

Fig. 5. Phosphorylation of H1 in the different phases of the cell cycle. HL60 cells were arrested in different phases of the cell cycle. Aphidicolin was used to block them at the G1/S transition, 5-fluorouracil for an S-phase arrest, and nocodazole to enrich M-phase cells as described in ''Materials and Methods.'' In addition, the uninduced (control) and cells with an 8 h topotecan treatment were used. The cell cycle profile was analyzed by flow cytometry (**A**). The percentage distribution in the different phases of the cell cycle is given by numbers in the graphs as described in Figure 4. H1 histones were extracted and subjected to CZE to analyze their phosphorylation state (**B**).

correlated with the appearance of the investigated apoptotic features, the DNA fragmentation and the caspase-3 activity (see Figs. 1 and 4). These results suggest that the dephosphorylations are not directly linked to the apoptotic process.

Previous analysis of the phosphorylation state of H1 and H3 histones after apoptosis induction has shown dephosphorylation as well as phosphorylation of these proteins depending on the cell line and on the agent used to induce apoptosis. A suppression of the H1 and H3 histone phosphorylation in murine ascites hepatoma cells by topoisomerase I inhibition with 10-hydroxycamptothecin was shown by Ling and Xu [1993], and Hendzel et al. [1998] described the absence of phosphorylated histones H1 and H3 in the apoptotic chromatin of PC12 cells. A dephosphorylation of H1 and H3 histones has also been observed after apoptosis induction of fibroblasts with TNF-α or anti-Fas antibody in combination with cycloheximide [Talasz et al., 2002]. These authors found that cycloheximide alone did not induce apoptosis but rapid H1 dephosphorylation, and they conclude that H1 dephosphorylation alone is not able to induce apoptotic chromatin alteration. Neither this nor any other investigation could correlate the observed histone dephosphorylation with the structural changes of the chromatin after apoptosis induction. Furthermore, several reports show a correlation of apoptotic chromatin changes and a phosphorylation of H1 and H3 histones. But these observed phosphorylations were probably side effects of the inducers which were either phosphatase inhibitors [Lee et al., 1999; Enomoto et al., 2001] or kinase activators, like cisplatin [Wang and Lippard, 2004] and the fungal toxin gliotoxin [Waring et al., 1997].

Due to the known relationship of the phosphorylation of the H1 and H3 histones to cell cycle phases, we studied the correlation between the cell cycle distribution and the state of histone phosphorylation after apoptosis induction with topoisomerase inhibitors. From our results, we can conclude that the dephosphorylation of the histones H1 and H3, which starts in the first hour after induction of HL60 and Jurkat cells with topoisomerase inhibitors, directly reflects the decrease of S- and M-phase cells. The rapid dephosphorylation of the H3 histones results from the decrease of M-phase cells through a G2 arrest, and the dephosphorylation of the H1 histones is more correlated to the decrease of cells in S-phase. The loss of S-phase cells is explained by the fact that HL60 cells exposed to topotecan or etoposide undergo S-phase selective apoptosis [Endresen et al., 1995; Huang et al., 2003]. The observed arrest of cells in G2 is a common feature induced in response to DNA damage, giving time to repair the DNA lesions. A G2 arresting effect of camptothecin, etoposide, and other topoisomerase inhibitors was also shown by other groups [Del Bino et al., 1990; Roberge et al., 1990; Del Bino et al., 1991; Dubrez et al., 1995], whereby the camptothecin induced arrest could be ascribed to the down regulation of cyclinB/cdc2 complex kinase activity [Tsao et al., 1992; Shao et al., 1997]. Mikhailov et al. [2004] showed that topoisomerase II inhibitors delay entry into mitosis, independent of ATM kinase by activation of the p38 MAPK checkpoint pathway.

On one hand, several investigations showed a dephosphorylation of H1 and H3 histones after apoptosis induction, especially with topoisomerase inhibitors; on the other hand, the cell cycle arresting effect of topoisomerase inhibitors is known and the mechanisms are partially elucidated. In the present study, we could prove a direct correlation of the dephosphorylation of the H1 and H3 histones with the changes in the cell cycle distribution as a result of treatment with topoisomerase inhibitors. In conclusion, investigations of apoptotic processes using cycling cells should always consider the effects of the apoptosis inducers on the cell cycle progression. However, even if the dephosphorylation of the H1 histones is a consequence of arresting the cell cycle progression and the specific loss of S-phase cells by the apoptotic process, we cannot exclude that this dephosphorylation is important for the apoptotic chromatin condensation and fragmentation.

ACKNOWLEDGMENTS

We are grateful to GlaxoSmithKline for providing topotecan.

REFERENCES

Ajiro K. 2000. Histone H2B phosphorylation in mammalian apoptotic cells. An association with DNA fragmentation. J Biol Chem 275:439–443.

Boggs BA, Allis CD, Chinault AC. 2000. Immunofluorescent studies of human chromosomes with antibodies against phosphorylated H1 histone. Chromosoma 108: 485–490.

Bradbury EM, Inglis RJ, Matthews HR, Sarner N. 1973. Phosphorylation of very-lysine-rich histone in Physarum polycephalum. Correlation with chromosome condensation. Eur J Biochem 33:131–139.

Bradbury EM, Inglis RJ, Matthews HR. 1974. Control of cell division by very lysine rich histone (F1) phosphorylation. Nature 247:257–261.

Cheng CH, Kuchta RD. 1993. DNA polymerase epsilon: Aphidicolin inhibition and the relationship between polymerase and exonuclease activity. Biochemistry 32:8568–8574.

Cheung WL, Ajiro K, Samejima K, Kloc M, Cheung P, Mizzen CA, Beeser A, Etkin LD, Chernoff J, Earnshaw WC, Allis CD. 2003. Apoptotic phosphorylation of histone H2B is mediated by mammalian sterile twenty kinase. Cell 113:507–517.

Del Bino G, Skierski JS, Darzynkiewicz Z. 1990. Diverse effects of camptothecin, an inhibitor of topoisomerase I, on the cell cycle of lymphocytic (L1210, MOLT-4) and myelogenous (HL-60, KG1) leukemic cells. Cancer Res 50:5746–5750.

Del Bino G, Skierski JS, Darzynkiewicz Z. 1991. The concentration-dependent diversity of effects of DNA topoisomerase I and II inhibitors on the cell cycle of HL-60 cells. Exp Cell Res 195:485–491.

Dubrez L, Goldwasser F, Genne P, Pommier Y, Solary E. 1995. The role of cell cycle regulation and apoptosis triggering in determining the sensitivity of leukemic cells to topoisomerase I and II inhibitors. Leukemia 9:1013–1024.

Endresen PC, Prytz PS, Aarbakke J. 1995. A new flow cytometric method for discrimination of apoptotic cells and detection of their cell cycle specificity through staining of F-actin and DNA. Cytometry 20:162–171.

Enomoto R, Koyamazaki R, Maruta Y, Tanaka M, Takuma K, Mori K, Lee E. 2001. Phosphorylation of histones triggers DNA fragmentation in thymocyte undergoing apoptosis induced by protein phosphatase inhibitors. Mol Cell Biol Res Commun 4:276–281.

Felsenfeld G, Groudine M. 2003. Controlling the double helix. Nature 421:448–453.

Goto H, Yasui Y, Nigg EA, Inagaki M. 2002. Aurora-B phosphorylates histone H3 at serine28 with regard to the mitotic chromosome condensation. Genes Cells 7:11–17.

Grant PA. 2001. A tale of histone modifications. Genome Biol 2:REVIEWS0003.

Hendzel MJ, Nishioka WK, Raymond Y, Allis CD, Bazett-Jones DP, Th'ng JP. 1998. Chromatin condensation is not associated with apoptosis. J Biol Chem 273:24470–24478.

Hohmann P, Tobey RA, Gurley LR. 1976. Phosphorylation of distinct regions of f1 histone. Relationship to the cell cycle. J Biol Chem 251:3685–3692.

Horn PJ, Peterson CL. 2002. Chromatin higher order folding: Wrapping up transcription. Science 297:1824–1827.

Huang X, Traganos F, Darzynkiewicz Z. 2003. DNA damage induced by DNA topoisomerase I- and topoisomerase II-inhibitors detected by histone H2AX phosphorylation in relation to the cell cycle phase and apoptosis. Cell Cycle 2:614–619.

Jenuwein T, Allis CD. 2001. Translating the histone code. Science 293:1074–1080.

Jordan MA, Thrower D, Wilson L. 1992. Effects of vinblastine, podophyllotoxin, and nocodazole on mitotic spindles. Implications for the role of microtubule dynamics in mitosis. J Cell Sci 102(Pt 3):401–416.

Kantarjian H. 1999. New developments in the treatment of acute myeloid leukemia: Focus on topotecan. Semin Hematol 36:16–25.

Khorasanizadeh S. 2004. The nucleosome: From genomic organization to genomic regulation. Cell 116:259–272.

Kratzmeier M, Albig W, Meergans T, Doenecke D. 1999. Changes in the protein pattern of H1 histones associated with apoptotic DNA fragmentation. Biochem J 337(Pt 2):319–327.

Kratzmeier M, Albig W, Haenecke K, Doenecke D. 2000. Rapid dephosphorylation of H1 histones after apoptosis induction. J Biol Chem 275:30478–30486.

Langan TA, Zeilig C, Leichtling B. 1981. Characterization of multiple-site phosphorylation of H1 histone in proliferating cells. Protein Phosphorylation 8:1039–1052.

Lee E, Nakatsuma A, Hiraoka R, Ishikawa E, Enomoto R, Yamauchi A. 1999. Involvement of histone phosphorylation in thymocyte apoptosis by protein phosphatase inhibitors. IUBMB Life 48:79–83.

Ling YH, Xu B. 1993. Inhibition of phosphorylation of histone H1 and H3 induced by 10-hydroxycamptothecin, DNA topoisomerase I inhibitor, in murine ascites hepatoma cells. Zhongguo Yao Li Xue Bao 14:546–550.

Longley DB, Harkin DP, Johnston PG. 2003. 5-fluorouracil: Mechanisms of action and clinical strategies. Nat Rev Cancer 3:330–338.

Loury R, Sassone-Corsi P. 2003. Histone phosphorylation: How to proceed. Methods 31:40–48.

Meergans T, Hildebrandt AK, Horak D, Haenisch C, Wendel A. 2000. The short prodomain influences caspase-3 activation in HeLa cells. Biochem J 349:135–140.

Mikhailov A, Shinohara M, Rieder CL. 2004. Topoisomerase II and histone deacetylase inhibitors delay the G2/M transition by triggering the p38 MAPK checkpoint pathway. J Cell Biol 166:517–526.

Norbury C, Blow J, Nurse P. 1991. Regulatory phosphorylation of the p34cdc2 protein kinase in vertebrates. Embo J 10:3321–3329.

Ormerod MG. 2000. Flow cytometry in the study of apoptosis. In Flow cytometry. New York: Oxford University Press. pp 235–248.

Pilch DR, Sedelnikova OA, Redon C, Celeste A, Nussenzweig A, Bonner WM. 2003. Characteristics of gamma-H2AX foci at DNA double-strand breaks sites. Biochem Cell Biol 81:123–129.

Prigent C, Dimitrov S. 2003. Phosphorylation of serine 10 in histone H3, what for? J Cell Sci 116:3677–3685.

Roberge M, Th'ng J, Hamaguchi J, Bradbury EM. 1990. The topoisomerase II inhibitor VM-26 induces marked changes in histone H1 kinase activity, histones H1 and H3 phosphorylation, and chromosome condensation in G2 phase and mitotic BHK cells. J Cell Biol 111:1753–1762.

Rogakou EP, Pilch DR, Orr AH, Ivanova VS, Bonner WM. 1998. DNA double-stranded breaks induce histone H2AX phosphorylation on serine 139. J Biol Chem 273:5858–5868.

Rogakou EP, Nieves-Neira W, Boon C, Pommier Y, Bonner WM. 2000. Initiation of DNA fragmentation during apoptosis induces phosphorylation of H2AX histone at serine 139. J Biol Chem 275:9390–9395.

Rogalinska M. 2002. Alterations in cell nuclei during apoptosis. Cell Mol Biol Lett 7:995–1018.

Shao RG, Cao CX, Shimizu T, O'Connor PM, Kohn KW, Pommier Y. 1997. Abrogation of an S-phase checkpoint and potentiation of camptothecin cytotoxicity by 7-hydroxystaurosporine (UCN-01) in human cancer cell lines, possibly influenced by p53 function. Cancer Res 57:4029–4035.

Shiio Y, Eisenman RN. 2003. Histone sumoylation is associated with transcriptional repression. Proc Natl Acad Sci USA 100:13225–13230.

Strahl BD, Allis CD. 2000. The language of covalent histone modifications. Nature 403:41–45.

Sugiyama K, Sugiura K, Hara T, Sugimoto K, Shima H, Honda K, Furukawa K, Yamashita S, Urano T. 2002. Aurora-B associated protein phosphatases as negative regulators of kinase activation. Oncogene 21:3103–3111.

Talasz H, Helliger W, Puschendorf B, Lindner H. 1996. In vivo phosphorylation of histone H1 variants during the cell cycle. Biochemistry 35:1761–1767.

Talasz H, Helliger W, Sarg B, Debbage PL, Puschendorf B, Lindner H. 2002. Hyperphosphorylation of histone H2A.X and dephosphorylation of histone H1 subtypes in the course of apoptosis. Cell Death Differ 9:27–39.

Th'ng JP. 2001. Histone modifications and apoptosis: Cause or consequence? Biochem Cell Biol 79:305–311.

Thornberry NA. 1994. Interleukin-1 beta converting enzyme. Methods Enzymol 244:615–631.

Tsao YP, D'Arpa P, Liu LF. 1992. The involvement of active DNA synthesis in camptothecin-induced G2 arrest: Altered regulation of p34cdc2/cyclin B. Cancer Res 52: 1823–1829.

Wang D, Lippard SJ. 2004. Cisplatin-induced post-translational modification of histones H3 and H4. J Biol Chem 279:20622–20625.

Waring P, Khan T, Sjaarda A. 1997. Apoptosis induced by gliotoxin is preceded by phosphorylation of histone H3 and enhanced sensitivity of chromatin to nuclease digestion. J Biol Chem 272:17929–17936.

Yamada K, Itoh R. 1994. Involvement of DNA polymerase delta and/or epsilon in joining UV-induced DNA single strand breaks in human fibroblasts (comparison of effects of butylphenyldeoxyguanosine with aphidicolin). Biochim Biophys Acta 1219:302–306.